ELSEVIER

Coordination Chemistry Reviews
211 (2001) 317–351

COORDINATION CHEMISTRY REVIEWS

www.elsevier.com/locate/ccr

Applications of luminescent transition platinum group metal complexes to sensor technology and molecular probes

J.N. Demas [a,*], B.A. DeGraff [b]

[a] *Department of Chemistry, University of Virginia, Charlottesville, VA 22904, USA*
[b] *Department of Chemistry, James Madison University, Harrisonburg, VA 22807, USA*

Received 14 September 1999; accepted 10 January 2000

Contents

* Corresponding author. Tel.: +1-804-9243343; fax: +1-804-9243710.
E-mail address: demas@virginia.edu (J.N. Demas).

PII: S0010-8545(00)00278-2

Abstract

Luminescent transition metal complexes are currently revolutionizing many areas of photochemistry and photophysics. In particular, they are proving useful as molecular probes and sensors. We discuss the design consideration in producing useful sensors and probes. As we show, complexes are amenable to rational design. Applications of inorganic complexes to a variety of sensor technologies are discussed. In addition, problem areas such as sensor–support interactions are covered.

Keywords: Luminescence; Sensors; Oxygen; pH; Molecular probes

1. Introduction

Long-lived excited state metal complexes are in the process of revolutionizing a number of areas of modern photochemistry and photophysics. In particular, platinum group metal complexes with α-diimine ligands have led to entirely new areas. Transition metal complexes (TMCs) have been used as photosensitizers in energy conversion and electron transfer [1], in chemi/electroluminescent systems [2,3], and as probes of heterogeneous binding and of dynamics [7] and macromolecular structure [4,5]. We will not discuss the enormous amount of information on excited state electron transfer reactions, potential applications to solar energy conversion, photocatalysis and electrochemistry, or macromolecular systems that are useful for energy harvesting [2,6,7]. Readers should consult the recent *Journal of Chemical Education* issue devoted to inorganic photochemistry and photophysics [8]. We focus on systems exhibiting luminescence and the applications of these luminescence properties to practical devices, in particular molecular probes and sensors.

The most studied of the luminescent complexes is the family of $Ru^{II}L_3^{2+}$ complexes (L = α-diimine), and they have proven particularly versatile in these applications due to their strong visible absorption, stability, efficient emissions, and long-lived excited states [9,10]. Further, their emitting state energies and excited state redox properties can be exquisitely sensitive to variations in the metal,

coordinating ligands, and local environment [11–14]. Many of these sensitizers exhibit a variety of energetically accessible charge transfer (CT), ligand field, and intraligand excited states that, having differing orbital parentage, can have quite different excited state characteristics. Since much photophysics and photochemistry is controlled by the lowest excited states [11], it is important to thoroughly understand excited-state energetics and dynamics. Such understanding allows the rational designing of new, more useful sensitizers and probes. Models of excited state behavior are based predominantly on the photophysics and photochemistry of the $*Ru(bpy)_3^{2+}$ and related sensitizers. Fig. 1 summarizes the ligand structures and abbreviations used here and shows a representative structure for one of our complexes. In addition to the extremely popular Ru(II) complexes, Os(II) [13,15], Ir(III) [16], Mo(0) and W(0) [17], and Re(I) [18–20] complexes are being studied with increasing interest.

TMCs can have many potential advantages as luminescence probes including long excited state lifetimes (τ values), which fall in the range 0.1 to >100 μs, and high luminescence quantum yields in the $0.01 \rightarrow 0.7$ range [21,22]. Many of them are easily excited in the visible with low-cost LEDs or inexpensive red diode lasers. They have large spectral shifts between the excitation and emissions, which minimizes the difficulty of isolating the excitation and emission wavelengths. Long τ values make lifetime measurements much easier than the typically low ns lifetimes of organic fluorophores. Long lifetimes allow efficient time discrimination from the ubiquitous background fluorescences. Importantly, the longer lifetimes also allow the excited state ample time to sample its environment and it is this interaction that makes these materials such sensitive reporters. We have found Re(I) probes which have luminescence quantum yields in room temperature (r.t.) fluid solutions of 0.4–0.7 with τ values >10–100 μs. Such extraordinarily high yields and long lifetimes make these molecules extremely attractive as molecular probes and in fluoroimmunoassay. Finally, properties such as the quantum yields, τ values, charges, shapes, and site selective binding can be systematically tailored by modifying the ligands or metal ions.

This paper is divided into three major sections. First, we will discuss the excited state properties of metal complexes with emphasis on d^6 systems and explain why these systems are actually amenable to rational design. The discussion on excited properties of metal complexes is adapted from our earlier article on the design and application of luminescent metal complexes [21]. Second, we discuss a number of sensors and applications based on these properties. Finally, while the area of luminescence TMCs is exceptionally promising, there are a number of unresolved issues and complexities that need to be worked through before these new systems achieve maximum utility.

2. States of metal complexes

We first examine the electron structures of TMCs and the correlation with their emission and absorption spectroscopy. Most TMCs have partially filled d orbitals

[23]. To a considerable extent the ordering and occupancy of these orbitals determines emissive properties. Fig. 2 shows a schematic orbital and state diagram for a representative octahedral MX_6 d^6 metal complex where M is the metal and X is a ligand that coordinates at one site. The d^6 notation indicates that the complex has six d-electrons; we focus on this configuration because of its central role in

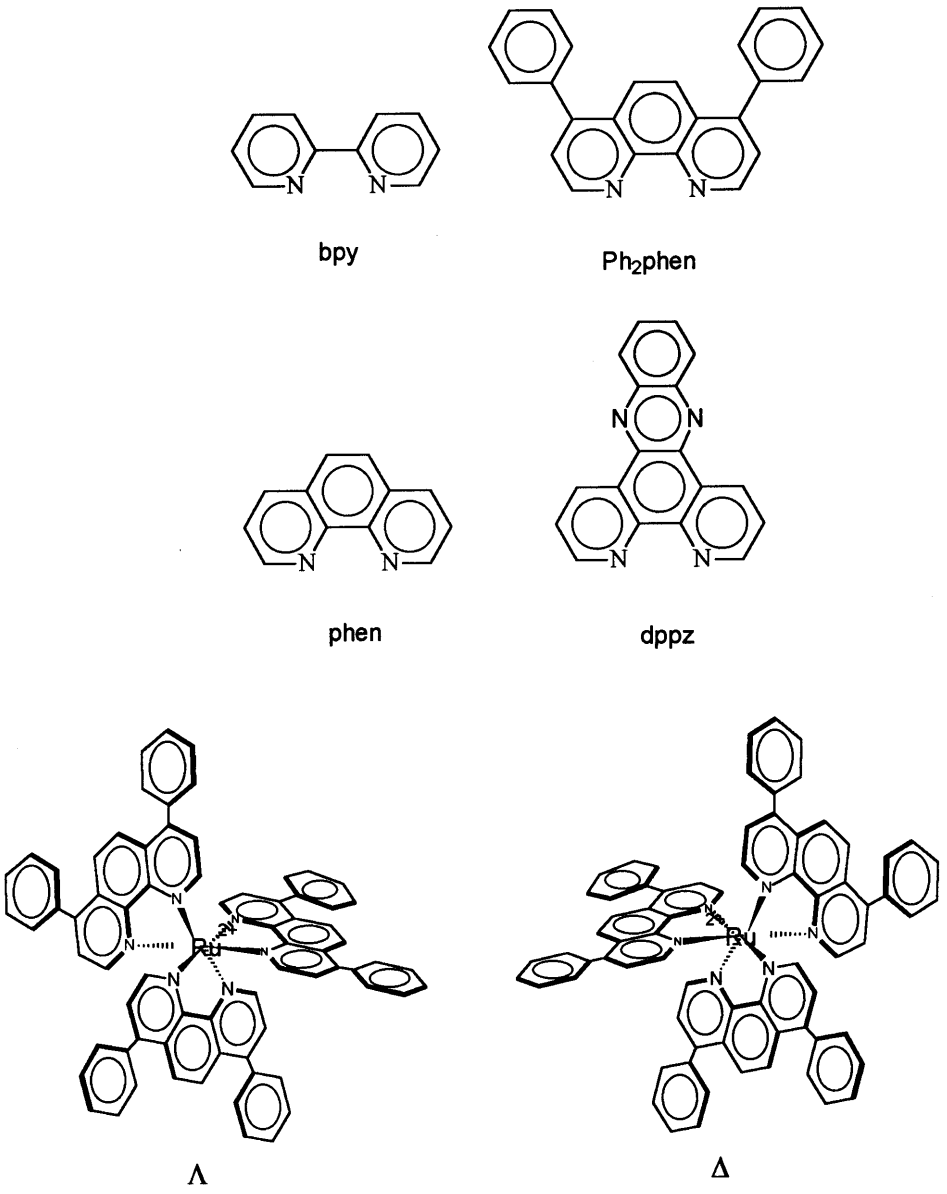

Fig. 1. Abbreviations for ligands used in this paper and a typical structure for a Ru(II) sensor–probe.

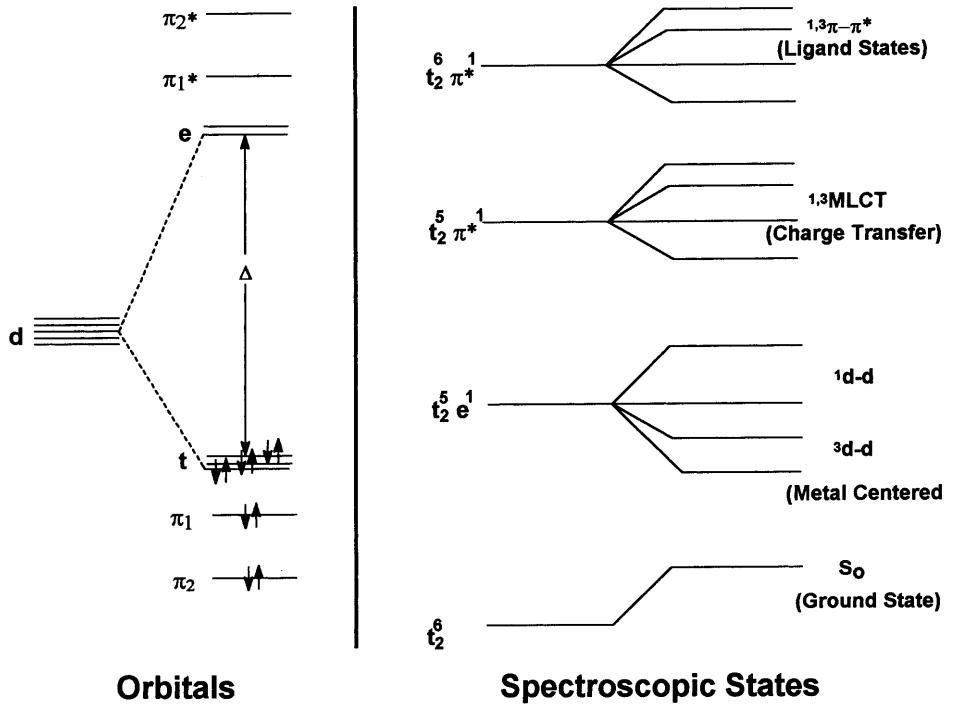

Fig. 2. Simplified orbital and state diagram for a d^6 metal complex in an octahedral environment showing the d and π bonding and antibonding orbitals. Each arrow represents an electron with its associated spin. A strong crystal field is assumed so that all the t_2 orbitals are filled. Ligand to metal charge transfer states are ignored.

current TMC luminescence. The octahedral crystal field of the ligands splits the degenerate five d-orbitals by an amount Δ into a triply degenerate t level and a doubly degenerate e level. The splitting arises from the different spatial orientations of the orbitals in relationship to the ligands. The two e-orbitals are directed towards the six ligands and the remaining t_2 orbitals point between the ligands. The different electrostatic interactions between the ligands and electrons placed in these different d-orbitals cause the splitting. Thus, an electron in an e-orbital is at higher energy than one in a t_2 orbital. The splitting magnitude is given by the crystal field splitting, Δ, which is a critical parameter for designing luminescent molecules. The size of Δ is determined by the crystal field strength of the ligands and the central metal ion. Altering the ligand, geometry, and metal ion can have a profound effect on luminescence properties.

Δ affects the distribution of electrons between the t_2 and e levels. If Δ is large (i.e. strong field), it is energetically more favorable to pair electrons in the t_2 level rather than to keep them unpaired by distributing them throughout the t_2 and e levels (Hund's rule). If Δ is smaller than the pairing energy, a weak field system results with the maximum number of unpaired electrons (four for a d^6 system). However,

weak field systems are not favorable for luminescence, and we do not consider them further. Only the strong crystal field case where all six d electrons pair and fill the t_2 orbitals is considered (Fig. 2).

The ligands have π and σ orbitals, but only the π orbitals are spectroscopically important for visible and near UV absorptions and emissions. There are both π bonding and π antibonding (π*) levels with all of the π bonding levels being filled.

The spectroscopic states are derived from the various orbital configurations (Fig. 2). In the ground state, all spins are paired, which makes it a singlet state. The lowest excited states are derived from promoting one of these paired electrons to an unoccupied orbital. The classifications of the resulting excited states are determined by the source and destination orbitals. There are three types of excited states: metal centered d–d states (d–d), ligand localized π–π* states (LL), and charge transfer states (CT). We use the standard notation that a d–d excited state arises by promoting a d electron within the d levels, a π–π* excited state arises by promoting an electron from a π bonding orbital to a π* antibonding orbital, and a charge transfer state arises either by promoting a d electron to a π* antibonding orbital or by promoting a π bonding orbital electron into an unfilled d orbital. In all of these cases, the excited states can be either singlets or triplets with the triplet state being lower in energy than its corresponding singlet state.

The lowest singlet and triplet ligand localized excited states are π–π* ones. These transitions are largely localized on the organic ligands and tend to be spectroscopically very similar to those of the free ligand, which is a consequence of the ligand localization. Fig. 3 shows the absorption spectrum of $Ru(bpy)_3^{2+}$ [24]. The intense high energy absorptions (250–310 nm) in $Ru(bpy)_3^{2+}$ and similar absorptions in related α-diimine complexes are spin allowed ligand-localized π–π* transitions; the spectral regions are very similar to those of the free α-diimine ligand showing the minor perturbation of the ligand localized π–π* transitions by the metal. Metalloporphyrins, especially with high atomic number Pt and Pd, can exhibit π–π* phosphorescences with high efficiencies and 100–1000 μs lifetimes. These have found applications in oxygen sensing [10].

Similarly, the lowest lying singlet and triplet d–d states arise from promoting a bonding t_2 electron to an e level to give a $t_2^5e^1$ configuration. As even spin allowed singlet–singlet d–d transitions are formally forbidden (Laporte forbidden), d–d transitions are characterized by low extinction coefficients (0.1–100), long radiative lifetimes, and high susceptibility to environmental quenching. Thus, most d–d emissions exhibit very low or negligible luminescence yields, especially at r.t. Additionally, the $t_2^5e^1$ configuration arises from promotion of a ligand bonding t_2 electron into a ligand antibonding or nonbonding e orbital. Thus, d–d states of $t_2^5e^1$ configuration tend to be reactive with respect to ligand substitution decomposition. Therefore, we are aware of no d–d emitting d^6 molecules that are likely sensors or probes. There are no discernible d–d transitions in $Ru(bpy)_3^{2+}$ type complexes, since the d–d transitions are too weak to be seen under the more intense charge transfer and π–π* transitions. Other electronic configurations, especially d^3 Cr(III) complexes, can give r.t. phosphorescences. Unfortunately, the combination of photochemical instabilities and low extinctions have prevented development of

sensors based on these systems. However, the Cr(III) ion in aluminum oxide (Ruby) is used as a high pressure sensor [25].

CT states involve both the organic ligand and the metal. In the systems under discussion, CT transitions arise from promoting an electron from a metal orbital to a ligand orbital ($t_2^5\pi^{*1}$ configuration) or from a ligand to a metal orbital (π^1e^1). The first are called metal-to-ligand charge transfer (MLCT) transitions and the second are ligand-to-metal charge transfer (LMCT) transitions. Since α-diimine ligands are easily reduced, we limit our discussion to only MLCT transitions. CT transitions tend to be more strongly allowed than d–d transitions; therefore, they have shorter radiative lifetimes and are less susceptible to intramolecular and environmental quenching. Also, the molar extinction coefficients of the spin allowed transitions are large (1000–30 000), which makes these CT states easier to pump optically. The intense 454 nm visible band of $Ru(bpy)_3^{2+}$ is an MLCT transition (Fig. 3).

Tetrahedral Cu(I) and square planar Pt(II) complexes also exhibit CT emissions in solution. The Cu(I) systems tend to have low luminescence quantum yields, which has restricted their use, but they have found use as DNA probes [26]. The Pt(II) systems can be more emissive and may find wider applications [27,28].

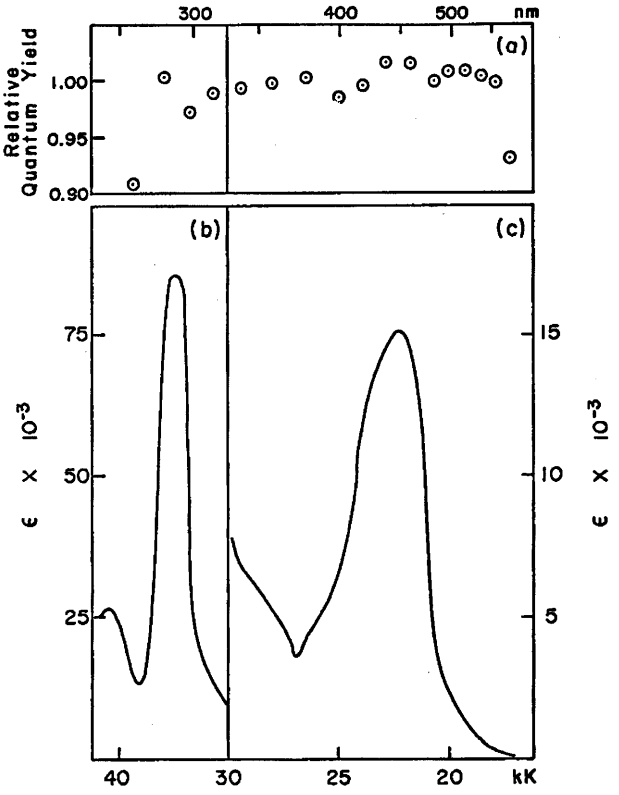

Fig. 3. Relative luminescence quantum yield (a) and absorption spectrum (b,c) of $[Ru(bpy)_3]^{2+}$. Note change in scale between b and c. Adapted from Ref. [24] with permission.

All currently used systems fail to match the ideal octahedral case of Fig. 2. All have lower symmetry, which further splits the d levels. However, it is still a reasonable model for discussion since the types of excited states present remain unchanged. While the octahedral Δ is no longer a rigorously meaningful quantity, d–d state energies are still dictated by the average Δ of all the ligands.

3. Design considerations

Knowledge of the above parameters allows synthetic control of the spectroscopy and, thus, luminescence properties. The chemist can alter the ligands, the geometry, and the metal ion. The most important design rule for luminescent TMCs is that the emission always arises from the lowest excited state. This rule derives from the general principle that radiationless decay from upper excited levels is very fast, and relaxation to the lowest excited level occurs with nearly 100% efficiency. This has been shown for $Ru(bpy)_3^{2+}$ and related complexes where the luminescence efficiency is independent of excitation into either MLCT or π–π^* excited states (Fig. 3). Fluorescence (spin allowed emission) is invariably absent in inorganic systems; this is a result of spin orbit coupling from the metal, which accelerates intersystem crossing to the triplet manifold. Thus, all major emissions in our systems arise formally from the lowest triplet state, and the emissions will be spin-forbidden phosphorescences. To first order, control of the luminescence properties of TMCs hinges on control of the nature of the lowest excited state and the energies and natures of the upper excited states relative to this emitting level.

Actually, the emitting CT levels are spin–orbit states with a large admixture of singlet and triplet character, and spin is probably no longer a good quantum number. Therefore, singlets and triplets are not good descriptors [29]. However, common usage is to refer to them as triplets and we will use this convenient notation.

The primary goals of sensor–probe design are the rational design of molecules that have high luminescence efficiencies and long excited state τ values, are easily pumped, have specific environmental sensitivity and binding properties, and are chemically and photochemically robust. Unfortunately, these aims can be mutually antagonistic. Based on a comprehensive body of experimental and theoretical work, the following important rules for meeting these criteria have been found to successfully guide the photophysical and photochemical properties of many inorganic complexes.

1. The lowest excited state must be either a CT or ligand π–π^*. This avoids photochemical instability associated with unstable d–d excited states.
2. A corollary to rule 1 is that the lowest d–d excited states must be well above the emitting level to avoid thermal excitation. Decomposition and rapid excited state decay are independent of how the d–d state is reached. Therefore, to maximize luminescence and minimize decomposition, the energy gap between the higher energy d–d state and the emitting state must be maximized.

3. Spin orbit coupling should be high to increase the emission allowedness and permit radiative decay to compete more effectively with radiationless decay. This largely precludes first transition series complexes.
4. Pure $\pi-\pi^*$ phosphorescences tend to be too long lived for efficient emission. Either spin orbit coupling or mixing with more allowed CT states must be used to increase the allowedness of $\pi-\pi^*$ phosphorescences. Re(I) systems can have $\pi-\pi^*$ and MLCT states, which are nearly degenerate; this class of systems can yield efficient $\pi-\pi^*$ or $\pi-\pi^*$-like emission (i.e. the emitting state has the energy and structure of a $\pi-\pi^*$ phosphorescence, but with a shorter lifetime) under probe–sensor conditions.
5. The emitting state cannot be too low in energy. The energy gap law states that radiationless processes become more efficient as the emitting state approaches the ground state [30,31].

We turn now to the chemical methods of realizing these goals. Critical is the removal of the destabilizing, non-emissive lowest d–d state from competition with the emitting level. The energies of the d–d states are controlled by varying either the ligands or the central metal ion to affect Δ. Stronger crystal field strength ligands or metals raise d–d state energies. Crystal field strength increases in the series.

$$\mathrm{Cl} < \text{pyridine (py)} \ll \text{bpy, phen} < \mathrm{CN} < \mathrm{CO}$$

Also, Δ increases by descending a column in the periodic table. As an added benefit, spin orbit coupling is most effectively increased by using higher Z metals.

These considerations immediately lead to the observation that suitable molecules will be rich in strong crystal field ligands such as α-diimines, CNs, phosphines, and COs. Further, optimal metals are likely to arise from the higher crystal field, high Z second and third transition series, rather than from the first row. Indeed, functional probe–sensors come from Re, Os, Ru, and Pt with major components of α-diimines, CNs, COs, and porphyrin ligands. We are unaware of any promising first transition series TMC. While it might seem tempting to place heavy atom substituents on the organic ligand to increase Z, this approach has proven much less effective than varying the metal and, in fact, may make the ligands more photochemically unstable.

Because CT transitions are generally of high intensity, have high luminescence potential, and can be tuned into the easily pumped visible region, they are frequently the lowest excited state of choice. CT state energies are affected by the ease of oxidation/reduction of the ligands and metal ion. Since α-diimines are easily reduced and Ru(II), Os(II), and to a lesser extent Re(I) are easily oxidized, complexes of this type with lowest MLCT states are common in TMC sensor–probe design.

The $\pi-\pi^*$ state energies are largely dictated by the ligands themselves. However, varying the substituents, heteroatoms in the aromatic portion, or the extent of π conjugation can all be used to alter the energies and intensities of the $\pi-\pi^*$ transitions or the environmental interactions so useful in sensor–probe design.

An example of the very detrimental effect of the energy gap law is shown in a series of $(bpy)ReX(CO)_3^+$ complexes (X = pyridine or substituted pyridine) [32]. The non-radiative decay rate, k_{nr}, varied dramatically with the MLCT emission maximum, which was controlled by varying the pyridine substituent. For the modest change in emitting energy of 2.2 k cm^{-1}, τ decreased from 0.96 μs (yellow emission) to 0.11 μs (red emission). Note also the ability to tune the emission over 2.2 k cm^{-1} merely by altering the pyridine substituents. Similar behavior occurs on going from yellow emitting Ru(II) probes with lifetimes in the 0.6–5 μs to deep red emitting analogous Os(II) complexes with 0.05–0.4 μs excited state lifetimes.

In our earlier article [21], we presented the apparently paradoxical emissive behavior of a series of TMCs and explained how they can be rationalized on the basis of the above simple rules derived from crystal field theory and simple quantum mechanics. For example, we show why the isoelectronic, isostructural series $Fe(bpy)_3^{2+}$, $Ru(bpy)_3^{2+}$, and $Os(bpy)_3^{2+}$ are totally nonemissive, moderately emissive, and somewhat emissive, respectively. We demonstrated why the similar appearing $Ru(bpy)_3^{2+}$ and $Ru(bpy)_2py_2^{2+}$ have completely different behavior. The former is quite emissive at r.t. while the latter is not only not emissive at r.t., but is photochemically highly reactive.

4. Sensors

4.1. Analysis strategies

We begin by describing different analytes and the strategies either currently in use or those likely to be used in the future for detecting and quantitating these analytes. There are several basic strategies used in luminescence detection. These include:

1. Specific bimolecular deactivation of an excited state by the analyte with a concomitant change in emission intensity or lifetime. Oxygen detection is an example.
2. Reaction of the ground or excited state species with the analyte to yield a species with different luminescence properties. Based on the degree of change of some property, one can quantitate the analyte. pH measurements are an example.
3. Variations on the previous cases include building a portion of the luminescence species that can react with the analyte and then quench or alter the luminescence properties. pH sensing is an example.
4. Incorporation of a non-luminescent, analyte sensitive molecule in a matrix that alters the luminescence of a transmitter species. By altering the deactivating or binding reactions of the non-emissive fragment with the luminescence species, the properties of the luminescent species can be altered and the analyte quantitated. pH sensing is an example.

Widely used luminescence methods of detection are emission intensity, spectrum, excited state lifetime, and emission polarization. We will give specific examples of each type of sensing strategy.

4.1.1. Quenchometric sensors

Quenching based sensors are based on the bimolecular quenching of excited states. The basic processes are:

$D+h\nu$	$\xrightarrow[k_1]{}$	D^*	excitation	(1a)
D^*	$\xrightarrow[k_2]{}$	$D+h\nu'$ or Δ	luminescence or deactivation	(1b)
D^*+Q	$\rightarrow$	$D+Q+\Delta$	catalytic deactivation	(1c)
		$D+Q^*$	energy transfer	(1d)
		$D^+ + Q^-$	oxidative electron transfer	(1e)
		$D^- + Q^+$	reductive electron transfer	(1f)

Several quenching modes are shown: oxidative or reductive quenching, energy transfer quenching, and catalytic deactivation of the excited state. The precise mechanism is irrelevant. The crucial factor is that some bimolecular processes will deactivate the excited state and reduce the emission intensity and excited state lifetime.

Provided that quenching is entirely diffusional (Eq. (1c–1f)), the excited state lifetimes and luminescence intensities are related to the quencher concentration by the lifetime and intensity forms of the Stern–Volmer equation

$$\tau_0/\tau = 1 + K_{sv}[Q] \tag{2a}$$

$$I_0/I = 1 + K_{sv}[Q] \tag{2b}$$

$$K_{sv} = k_2\tau_0 \tag{2c}$$

where τ and I values are luminescence lifetimes and intensities, respectively. The subscript '0' denotes the measurement in the absence of quencher. K_{sv} is the Stern–Volmer quenching constant, and k_2 is the bimolecular quenching constant. Ideally, plots of τ_0/τ or I_0/I versus $[Q]$ will be linear with identical slopes of K_{sv}.

4.1.2. Excited state reactions

Fig. 4(A) shows a typical scheme for detection of an analyte by reaction of the luminescent reagent R* with the analyte A to form a new excited state species RA*. If RA* has different emission characteristics than R*, these differences can be used to quantitate A. The best developed systems measure pH by reaction of the analyte, a proton H^+, with the conjugate base B^{*-} to form HB*. While ground state methods based on absorption could be used, they lack sensitivity and are inadequate when a few μl of sensor chemistry are used at the end of a fiber optic probe.

There are several important points. Because of the large excited energies of electronic excitation and the different electronic configurations between the ground and excited states, K and K^* do not have to be the same. Indeed, they are frequently different. The limiting case is excimer or exciplex formation where the excited state complex has no counterpart in the ground state.

A variation on this scheme is shown in Fig. 4(B). A reagent is covalently attached to the luminescence portion of the molecule through an electronically non-conducting link such as a CH_2–. The alteration of environment near the excited state

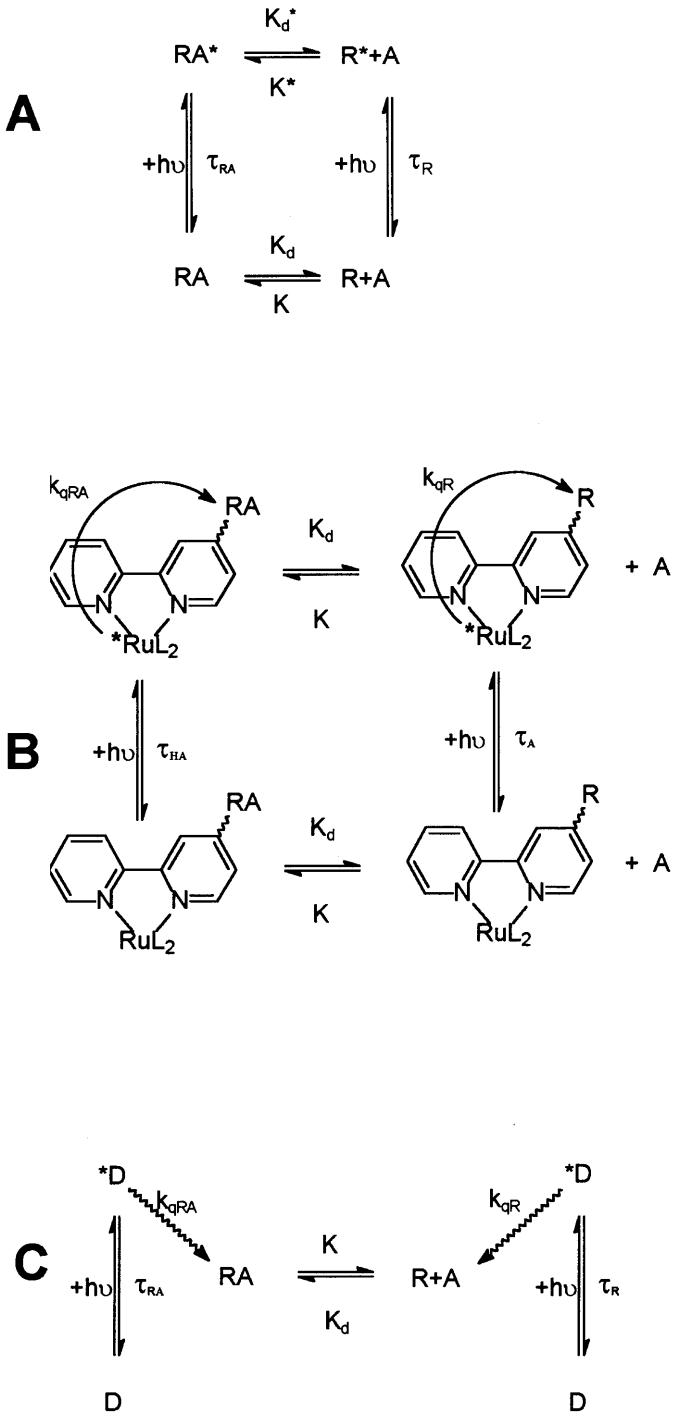

Fig. 4. Various strategies used to measure an analyte A by luminescence.

changes the luminescence properties and can be used to signal reaction with the analyte. The original idea was to use a species with redox properties altered by the analyte. If the analyte changed the redox species from or to a quencher, the varying degree of quenching with or without the analyte present would allow quantitation. In practice, things have proved more complex with what should be the most heavily quenched species exhibiting the greatest luminescence. Charge and exciplex formation have been suggested explanations [33].

4.1.3. Long range energy transfer

Another clever quenching based scheme utilizes long range dipole–dipole energy transfer (Fig. 4(C)). If an energy acceptor molecule has an intense absorption that overlaps strongly with the emission of a donor molecule, then efficient long range quenching of the donor can occur without diffusional contact. The transfer can occur at up to 90 Å in favorable cases. The major requirement for sensor application is that there be a significant difference in the absorption spectrum of the reagent R and its complex with the analyte, RA. It is also necessary to engineer the system so that the donor–acceptor distances are appropriate for different rates of energy transfer from donor to the two different acceptors.

4.1.4. Polarization

In many cases there is no discernible change in the emission wavelength or lifetime on binding of the analytes. However, in the case of antigens binding to antibodies there can be large changes in molecular weight, and these changes can translate into variations in the rotational correlation times of the complex relative to the separate components. Time-resolved luminescence polarization measurements allow direct measurement of the rotational correlation time [34]. This approach forms the basis of a number of fluoroimmunoassay methods and the study of the dynamics of macromolecules (vide infra).

5. Examples

5.1. Oxygen sensors

Current oxygen sensors are based on bimolecular quenching as given in Eqs. (1 and 2). In the case of oxygen quenching of metal complex excited states, the primary quenching mechanism seems to be energy transfer to form singlet oxygen. Wolfbeis has an excellent review [35], and we have recently discussed oxygen sensors and their applications [10].

Oxygen deactivation or quenching of excited states has been recognized since the early days of luminescence. It has generally been a nuisance and needed to be removed to permit luminescence to be observed. Frequently, it was such a severe problem that it would preclude luminescence measurements unless the most extreme deoxygenation methods were used. However, detection and quantitation of oxygen is an exceptionally important area in industry and in the biomedical field. While the

potential of quenchometric quantitation of oxygen was recognized relatively early, only recently have commercial systems utilized it.

Since the excited states of many species that can be quenched by oxygen are sensitive to environment and will respond to metal ions, oxidants, reductants, surfactants, DNAs, proteins, etc., the key to practical systems is separating the sensor molecule from all the interferents while still allowing access to oxygen. The simplest and most widely used approach is to put the sensor into a gas permeable, solvent impermeable membrane. Some of the most successful sensors have been based on silicone elastomers since the basic polydimethylsiloxane structure can have excellent oxygen diffusion and quenching with the added benefit of good biocompatibility.

Because of their long excited state lifetimes, large shifts between excitation and emission, and efficient emissions, metal complexes have become important oxygen sensors, particularly $[Ru(Ph_2phen)_3]^{2+}$ [36,37]. Fig. 5(A) shows a Stern–Volmer plot for $[Ru[Ph_2phen)_3]^{2+}$ immobilized in a silicone rubber, in this case GE RTV-118, a bathtub caulking compound. The excellent sensitivity of this system over the physiologically interesting range of 0–1 atm of oxygen is apparent. The emission intensity decreases by about a factor of 8 on going from no oxygen to an atmosphere of air and by a factor of 25 at an atmosphere of pure oxygen. These dramatic changes are easily quantitated. $[Ru(Ph_2phen)_3]^{2+}$ forms the sensor element in at least one commercial system used for on site, near real time monitoring of critical care patients.

The Stern–Volmer quenching plot is nonlinear. This non-linearity is characteristic of solid state supports as opposed to solution where the linear behavior predicted by theory is generally rigorously observed. The non-linearity appears to be a consequence of the heterogeneity in the polymers. This heterogeneity is a result of the sensor molecules existing in two or more sites with different quenching constants. Such heterogeneity will always result in downward curved Stern–Volmer plots. This particular case has relatively little heterogeneity. Much larger values are observed with other probes even in the same polymer. We return to this issue later.

A nice demonstration of the sensitivity is given in Fig. 5(B) where a sensor film is being breathed over. At one point, the subject held his breath and then resumed breathing. The sensitivity of the luminescence intensity to O_2 is quite evident. Note, in particular, the large burst in emission intensity (lower O_2 concentration) after he held his breath (a result of the greater exchange time in his lungs); the irregularities of the next first few breaths due to the higher CO_2 levels in the blood; and, ultimately, the restoration of the equilibrium oxygen concentration. We have described a dramatic demonstration of luminescence oxygen quenching that would be useful as a teaching aid [38].

5.2. pH sensors

Absorption spectroscopy has long been used for measuring pH. Changes in the absorption spectra for species having pH dependent ground state chemistry can be used as both quantitative pH determinations and as titration end point detectors.

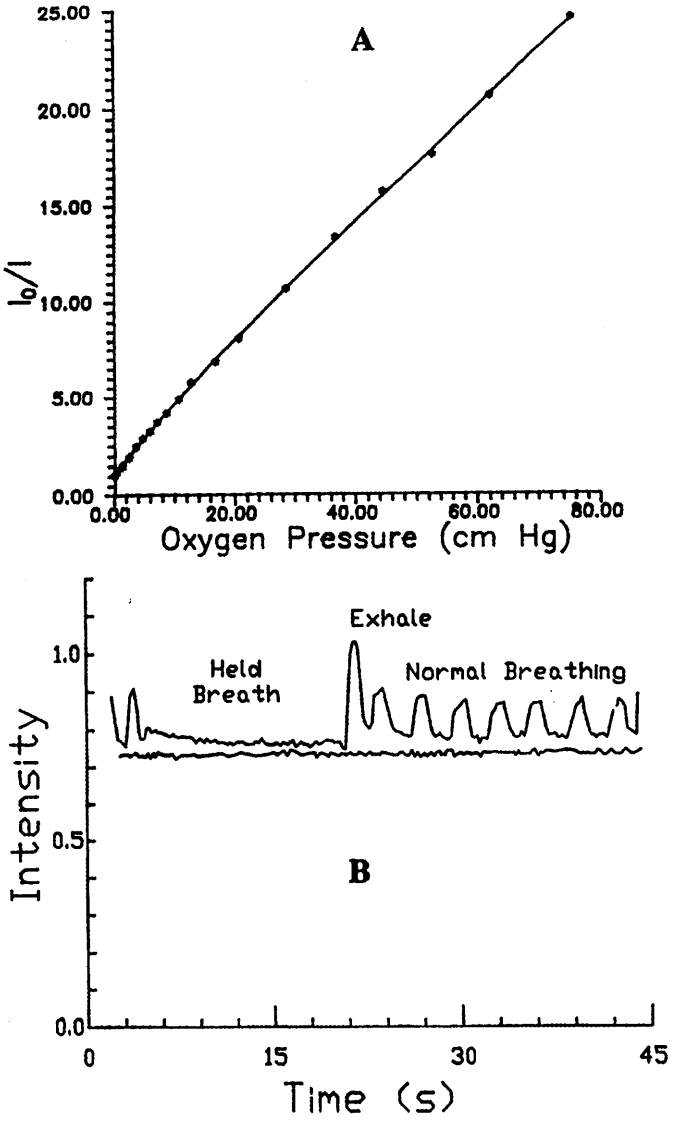

Fig. 5. (A) Intensity Stern–Volmer quenching plot for $[Ru(4,7\text{-}Ph_2phen)_3]^{2+}$ in silicone rubber [37]. The solid line is the best fit for a two-site model (Eq. (7)) with different quenching constants. (B) Luminescence intensity of $Ru(4,7\text{-}Ph_2phen)_3^{2+}$ in silicone rubber while being breathed over [36]. Copyright 1991 and 1987 American Chemical Society.

Absorption spectra are insensitive, which increases the difficulty of using them with very small sensors. However, luminescent molecules that show pH dependent changes in luminescence spectra with changes in pH can be used as luminescence pH indicators. The simplest approach is to use differences in the luminescence properties of the acid and its conjugate base.

An easy scheme for measuring pH is excited state acid–base chemistry. This is an example of Fig. 4(A) where H^+ would be the analyte and R^- would be the conjugate base of HR. K and K^* do not have to be the same and, in general, are different. The reason for this difference is that the excited state molecules can be thought of as completely different molecules from the ground state molecule. The excited state molecule has substantially more energy (190 kJ mol^{-1} or greater for a visible emitting species), and the excited state will generally have a completely different electron distribution from the ground state. Both of these factors can cause pK^* to differ from pK. In some cases the pK values can differ by 5–10 pK units. This would be equivalent to converting an acid of the strength of acetic acid into a nonacid or a super acid.

The first example reported for an excited state acid base reaction of a platinum group metal diimine complex was for $RuL_2(CN)_2$ [39]. The two cyanides can be protonated at the N end, which dramatically blue shifts the MLCT excited states. The two pK values are on the order of 0–1. However, on excitation the complex becomes a super acid with a highly negative pK. While fundamentally very interesting, these complexes are not interesting for monitoring pH values in the range of greatest interest ($5 < pH < 9$), although they may have some utility in the extreme acidity range of much less than 0.

One does not necessarily expect the usable range for an indicator in the ground state to be the same as if the ground state species were used as an indicator. For example, with $Ru(3,4,7,8\text{-}Me_4phen)_2(4,7\text{-}(HO)_2\text{-}phen)^{2+}$, the pH titration curve using ground state absorption has a break at 5 while the excited state emission titration curve has a break at pH 2 [40].

There is an alternative approach to emission pH sensing. The technique involves building a composite molecule that has a luminescent piece, which is covalently attached to a fragment that is pH sensitive and can quench the excited portion differently depending on its state of protonation. The most common version of this type of sensor uses electron transfer quenching since the redox potentials of many species are dependent on their state of protonation. Thus, depending on whether a species is protonated, it can act as a quencher in one form and a nonquencher in the other. This is shown schematically in Fig. 4(B).

Examples of such built-in quenching systems involve α-diimine ligands with CH_2 coupled pendant phenol groups where the phenolate ion is a much more efficient electron transfer quencher than the phenol [33]. The usable pH range of this system is about 6–10. Another example includes $-CH_2NR_2$ groups since amines can be good reductive excited state quenchers of RuL complexes [41]. A variation on this mechanism is where the Ru(II) emission shows a pronounced variation in emission characteristics with the charge on the pendant groups. These systems are usable in the 0–8 pH range [41].

Fig. 6 shows a titration curve for a diamino Ru(II) complex supported on a polymer [42]. These data reveal two important issues. The double hump clearly indicates the presence of more than one pK^*, which is not surprising given the two basic nitrogens. However, in solution, one of the two pK^* values is at 7.5, which would suggest that it would be perfect for physiological measurements. Inspection

of the polymer supported titration curve reveals that the pK^* has shifted substantially to more basic regions, and the polymer supported sensor is not suitable for physiological measurements. This result once again demonstrates that the transfer of solution data to polymer systems is not always smooth and many surprises will occur.

Another possible mechanism would be from pendant groups (Fig. 4(B)) that can fold back and form intramolecular exciplexes (**exci**ted state com**plex**) between the excited species and the redox active part. Under these conditions, both the intensity and spectrum could change with pH.

A final strategy for pH sensing is the indirect quenching approach. This depends on the fact that very efficient dipole–dipole resonance energy transfer can occur between an excited donor and a ground state acceptor molecule if the emission of the donor overlaps well with a strong absorption band of the acceptor. The noncontact energy transfer mechanism is called Förster energy transfer after Th. Förster [34,43] who is responsible for working out the details for molecular systems in solution. The key features of Förster transfer are that it does not involve contact and therefore does not need diffusion, can occur at 30–90 Å separation, and has rates competitive with short lived fluorescences. A schematic representation is shown in Fig. 4(C). The sensor contains a pH sensitive dye (HA), and HA and A^- have different spectra with significantly different overlaps with the emission of the luminescent donor, D. As the pH is varied, the fractions of dye in the different

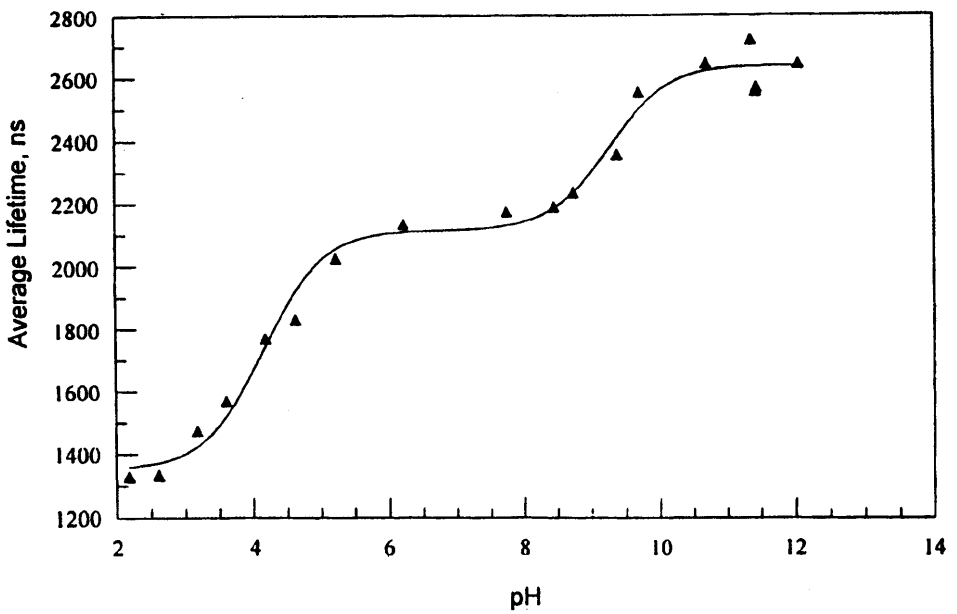

Fig. 6. Lifetime pH titration curve for polymer immobilized $[Ru(Ph_2phen)_2(DEAM)_2bpy]^{2+}$ ($(DEAM)_2bpy$ = 4,4′-bis(diethylamino)methyl-2,2′-bipyridine) in air-saturated water. The solid line is the two pK^* fit to the data. Adopted with permission from Ref. [38].

forms vary and the rate and efficiency of quenching of *D varies with pH. One can monitor the emission intensity or the lifetime. However, unlike oxygen quenching, which, at least in solution, gives single exponential decays, Förster quenching kinetics are highly non-exponential.

A good variation on pH sensing utilizes the Förster mechanism of Fig. 4(C) [44]. Protonation of a pH sensitive dye changes its absorption spectrum. By proper selection of the dye, the absorption emission overlap of the donor and acceptor vary and the degree of quenching of the donor changes. The problem with this approach is how to organize it so that the pH sensor energy acceptor is always maintained at a suitable distance from the donor. This problem can be largely overcome by making the donor and the acceptor an ion pair. In principle, this ion pairing automatically maintains the donor and acceptor at a suitable interaction distance. In practice, the response of the sensor has shown a strong dependence on concentration, which suggests that there is not complete association in the sensing environment.

This energy transfer approach has also been modified to produce a chloride ion sensor [45]. A $[Ru[Ph_2bpy)_3]^{2+}$ donor is used in conjunction with a bromothymol blue anion as the indicator. Since the dye has a pK of 7.5 it works in the physiological range. The sensor ion pair is supported in a hydrophobic membrane. Coextraction of a proton from the aqueous phase along with the chloride counter ion into the membrane provides a proton to change the more highly quenching blue form of the dye into the less quenching yellow protonated form. The luminescence of the ruthenium complex is monitored by changes in the apparent lifetime using a phase shift measurement or by intensity methods. Because of the long lifetimes of the ruthenium complex, phase measurements are inexpensive and low cost blue LEDs can be used as the excitation source.

The response is pH and ionic strength dependent, so these parameters must be controlled in the analysis. At $pH > 7$, severe photodecomposition possibly due to singlet oxygen generation is a problem. Depending on pH, the working range is 0.5–200 mM.

5.3. Carbon dioxide and ammonia sensors

Until recently the majority of CO_2 sensors were actually pH sensors [46]. A carbonate–bicarbonate buffer is separated from the analyte fluid by a CO_2 permeable membrane. The pH of the buffer changes in response to the CO_2 concentration in the analyte fluid. Then, a pH sensitive fluorescent dye is used to track the pH of the buffer and this, in turn, allows the CO_2 concentration to be inferred. The problem of using metal complexes in this system then reduces to getting a good pH sensor in the correct pH range. The development of such sensors is still in its infancy, but there is little doubt that long-lived pH sensitive metal complexes will prove useful in this area.

An alternative approach is based on energy transfer to a pH sensitive dye in polymer systems. Very fast responding colorimetric CO_2 sensors based on pH sensitive organic dyes have been demonstrated [47].

$$\{D^+Q^-\ xH_2O\} + CO_2 \overset{\alpha}{\leftrightarrow} \{D^+HCO_3^-\ (x-1)H_2O\ HQ$$

The curly brackets indicate an ion pair in a hydrophobic matrix. The water is carried along with the ions. Q^- denotes the conjugate base of the acid HQ. If the pK is correctly chosen, carbon dioxide will react with the water and with Q^- to convert it into HQ. If Q^- and HQ have *significantly* different absorption spectra that overlap with emission of D, then a nice Förster quenching based sensor can be produced (Fig. 4(C)). This system is identical to the resonance based pH sensor described above, but has less stringent requirements. Unlike the pH sensor, the polymer needs only to be permeable to CO_2 and not the water of the aqueous media. This reduces the need for some type of covalent or ionic attachment of the components to the support in order to avoid leaching problems.

Similar strategies can be used for ammonia [48]. Although there does not yet appear to be an ammonia system based on quenching of the luminescence of a metal complex, all of the necessary features are present.

5.4. Specific metal ion sensors

Sensitive, specific metal ion optical sensors are among the highest goals of optical measurements. Perhaps the most significant area is in biomedical applications. Ions of interest include sodium, potassium, calcium and magnesium. Such technologies are invaluable in clinical analyses and in such areas as in-vivo imaging of cellular components in living cells viewed under fluorescence microscopes. The key here is to configure the complex so that selective association of the analyte metal occurs with the metal complexes and yields a distinguishable change in luminescence.

Ruthenium(II) complexes, for example, have shown a high tendency to form characteristic exciplexes or new luminescent metal complexes with Ag^+. $Ru(II)L_3$ complexes form 1:1 and 1:2 exciplexes with silver [49]. Probably more useful is that $RuL_2(CN)_2$ complexes will form more highly luminescent complexes with silver via a Ru–CN–Ag structure [50]. Since these emissions of the Ag–cyano complexes are blue shifted over the parent complex, good analytical performance seems likely. There are two problems with these systems. The binding constants are not large enough for high sensitivity. Also, certain other metal ions can quench the excited states (e.g. Cu(II), Fe(III)), and a variety of metal ions can compete for the available CN binding sites [51].

Much more specific systems would be ones that contain a highly selective component that binds selectively to the analyte. Examples of intrinsically selective groups are crown ethers, cyclodextrins, and specific multidentate ligands such as in the calcium sensitive probes. This work is still in its infancy; Re(I) based systems with a crown ether were recently reported, although they responded to a variety of divalent ions such as Zn and Ca as well as K [52]. A cyclam bipyridine containing Ru(II) complex has been prepared for use as a metal ion detector [53]. Once quenching ions such as copper are bound to the cyclam they appear to totally quench the luminescence, but the cyclam ion complex may form too slowly and bind too strongly to permit its use as an analytical tool.

5.5. Temperature sensors

The significant and predictable temperature dependence of the emission of metal complexes suggests their use as temperature probes, although to our knowledge no one has actually used them in such applications. In particular, Crosby suggested Ru diimine complexes as cryogenic sensors. These complexes have very large temperature coefficients below liquid nitrogen temperatures and huge coefficients at liquid helium temperatures. For example, the luminescence lifetime of $Ru(bpy)_3^{2+}$ changes from 5 to 200 μs on going from 77 to 4 K [54]. Their multi-microsecond lifetimes and ease of excitation with blue LEDs should make them superb remote cryogenic sensors.

In view of the great difficulty of controlling sample temperature at cryogenic temperatures, particularly in cold finger arrangements, the Crosby sensors would appear to be attractive for measurement probes. For example, it would be very easy to paint a cold finger probe with the complex in a polymer. Then, by interrogating the lifetime at different positions, the temperature profile across the device could be easily measured. By using a focused laser beam, a resolution of a 100 μm or less should be possible. Alternatively, using an optical imaging system, the entire temperature profile of a device could be measured at once. Of course, this approach is also possible at room or elevated temperature.

Especially in the cryogenic supersonic wind tunnel where both pressure and temperature are important parameters, metal complexes are attractive temperature sensors. $[Ru(terp)_2]^{2+}$ is not luminescent at r.t., but glows brightly at low temperatures. This feature makes it the basis of temperature sensitive luminescence paints. By suitable modification of the complex, the temperature range over which it can respond can be altered.

However, even at r.t. the temperature coefficient is large enough to be very reasonable. Based on the thermal quenching via only an upper d–d level, we have carried out a theoretical analysis on the molecular parameters of a sensor molecule for optimizing sensor response for different temperatures [55]. The model is very attractive for predicting behavior and designing systems for use in the liquid nitrogen (77 K) to above ambient (ca. 350–450 K) temperature range. This model is inappropriate for the low temperatures of Crosby's measurements where two or three closely spaced sublevels of the emitting state manifold are involved.

5.6. Immunoassay and bioprobes

In most clinical laboratories, with the exception of a few simple metal ion analyses, the most common methods of analysis are based on immunoassay methods [56]. The procedure for immunoassay consists of having an antibody, Ab, which is specific for the desired analyte that is an antigen, Ag, for the antibody. The antigen is labeled, Ag–D. If Ag–D is added to Ab, it will bind to form a tagged complex Ab···AgD, where the ··· stands for a non-covalent bond, which nevertheless can be quite strong.

$$Ab + AgD \leftrightarrow Ab\cdots AgD \quad (3)$$

Now if the analyte is added to the solution, it will competitively bind with the antibody and displace the labeled antigen.

$$Ab\cdots AgD + Ag \leftrightarrow Ab\cdots Ag + AgD \quad (4)$$

If an analysis can be developed to determine the amount of AgD bound to Ab as a function of the analyte concentration, Ag, then an Ag analysis is available. Since antibody antigen reactions can be made exquisitely selective and with useful strong binding constants, immunoassay provides a powerful general method of analysis. This is particularly true since antibodies can now be readily produced for a wide variety of antigens.

The original approach to immunoassay used radioisotopes. This is slow and, with the waste disposal problems, alternative methods have been sought. Because of the exceptionally high sensitivity possible with luminescence, it has become the method of choice. Subsequent discussions are limited to luminescence based methods.

The key then is to develop methods for measuring the ratio of bound to unbound AgD. In principle, if binding directly alters the luminescence properties, a method is available. However, the probe and the binding site should generally not be too close and interact or the specificity of the binding can be altered.

There are two better approaches. The first is polarized luminescence immunoassay [57]. One can monitor the fluorescence polarization of AgD in the solution. Emission polarization of molecules depends on their rotational correlation times compared to their emission lifetimes. Since large molecules tumble more slowly than small molecules, larger molecules will exhibit more polarized emissions than smaller molecules with the same emission lifetime. In the above equilibria (Eq. (4)), the polarization of the AgD emission will decrease as it is displaced from Ab···AgD by adding increasing amounts of the competitive binder Ag.

The second approach is based on luminescence energy transfer [58]. The antibody is labeled with a quencher, Q, for D. The critical equilibrium is then

$$Q\text{–}Ab\cdots AgD + Ag \leftrightarrow Q\text{–}Ab\cdots Ag + AgD \quad (5)$$

In the antibody-bound AgD, the emission of D is partially or completely quenched by the quencher Q on Ab. The average lifetime and intensity of D will then depend on the amount bound to Ab. This lifetime or intensity signal can then be translated into the amount of Ag in solution.

The simplest and most reliable form of quenching is Förster resonance energy transfer. This does not require any contact between the probe and the quencher, which avoids the need for contact interactions that can interfere with binding specificity.

Lakowicz and coworkers have demonstrated applications of Ru(II) complexes in both dynamic luminescence depolarization [57] and resonance energy transfer [58] immunoassay. The long lifetimes of metal complex luminophores increases the molecular weight limit of detectable analytes from less than several thousand for a typical 4 ns lifetime probe to $> 10^6$ for a 400 ns Ru(II) probe. For resonance energy

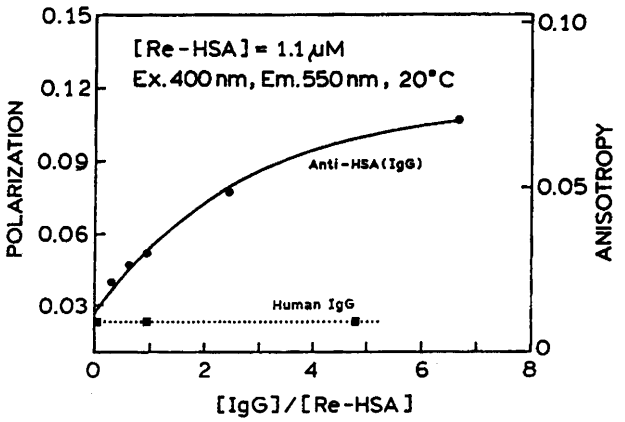

Fig. 7. Steady-state fluorescence polarization of a Re(I) labeled horse serum albumin (Re–HSA) at various concentrations of IgG specific for HSA (anti-HSA, solid circles). The selectivity is shown by the absence of a response to Human IgG (squares). Both anisotropy and polarization are shown. Adapted from Ref. [59] with permission.

transfer methods, the long excited state lifetimes greatly simplify the lifetime measurements. Also, ruthenium complexes are highly attractive because they can be excited with inexpensive blue LEDs.

Fig. 7 shows the result for a polarization based fluoroimmunoassay utilizing a Re(I) complex [59]. Both specificity and sensitivity of the method are demonstrated. This elegant approach is likely to prove the basis for a wide range of practical devices.

6. Molecular probes

6.1. Chirality and conformational probes

A fertile area is elucidating the nature and dynamics of small molecules binding to DNA. In particular, the design of site/conformation specific probes [60], selective cleaving agents for mapping and fingerprinting [61], and the potential of directed drug design [62] drive this work. Traditionally, work has focused on small intercalative binders, usually heterocycles with extended π system and high DNA affinity (e.g. ethidium bromide, acridine orange) [63,64].

Recently metal complexes have shown promise as site-conformation specific binders and catalytic cleavers. Although much work has been done on planar Pt(II) complexes, some of the most interesting recent work has used octahedral Ru(II) complexes with α-diimine ligands pioneered by Barton et al. [65–68]. These complexes are homo- or heterochelated complexes of the form $Ru^{II}(LL'L'')$ where $L = L' = L''$ for the homochelated case. In general, the L values are α-diimine ligands such as bpy, phen, their substituted analogs, or analogous heterocycles with

the nitrogens replacing aromatic carbons. For sufficiently extended π systems, the α-diimine may bind in the major groove of the DNA helix by intercalation of one ligand into the base pair stacking. The remaining two ligands sterically interfere with the phosphate backbone and block full insertion.

Since the metal complex is trigonal, it exists in Λ and Δ enantiomeric forms (shown in Fig. 1 for $Ru(Ph_2phen)_3^{2+}$). The Λ isomer experiences less severe steric crowding than the Δ isomer on intercalation into the helical optically active DNA duplex, which causes tighter binding for the Λ isomer and a higher affinity [65–68]. This feature is used to probe different DNA conformations. To date, considerable work has been done on these Ru(II) systems with a variety of α-diimine ligands. Important conclusions are:

- Ru(II) complexes make nearly ideal probes because of the long τ values (0.1–10 μs), bright luminescences, and variable excited state redox properties for DNA nicking. Their emissions allow use of a wealth of luminescence techniques (e.g. emission shifts, polarization, and selective excited state quenching).
- Large hydrophobic ligands are required to obtain specific intercalative binding versus a non-specific ionic binding. Intercalative binding is required for chiral recognition. Selectivity goes as follows: $Ru(bpy)_3^{2+} \ll Ru(phen)_3^{2+} < Ru(Ph_2phen)_3^{2+}$ [65–68]. For smaller ligands such as phen, there was controversy over the precise binding mode [69], although for the phen, binding is probably not intercalative [70].
- Chiral recognition occurs with B–DNA but not Z–DNA. Barton suggested using Λ isomers to identify Z–DNA regions; the Λ isomer does not bind to B–DNA but does to Z–DNA [66].
- Single stranded DNA binds electrostatically and shows little chiral recognition [71].
- Highly reducing excited states photocleave DNA at guanine. O_2 quenching is less specific [72,73].

A ligand that has been especially popular is dppz (Fig. 1), which is known as the 'molecular light switch' [74]. The nitrogens in the extended anthracene-like structure can couple strongly to water and quench excited states. For example, $Ru(bpy)_2dppz^{2+}$ and $Ru(phen)_2dppz^{2+}$ are essentially nonluminescent in water yet highly emissive in solvents like CH_2Cl_2. On formation of a complex with DNA, the dppz intercalates much more strongly between the base pairs than phen or bpy. The inclusion region is very hydrophobic, protects the nitrogen lone pair electrons from water, and simulates a nonaqueous environment, which allows the complexes to emit reasonably efficiently. Even with $Ru(phen)_2dppz^{2+}$ there is controversy about whether binding is intercalative in the major or the minor groove [75].

Because of this unique ability, dppz has been suggested as a molecular dip stick for probing local nonaqueous environments. Unfortunately, it fails in such simple systems as cyclodextrins (CDs). In $Ru(phen)_2dppz^{2+}$, one would have expected the dppz to go into the hydrophobic cavity and turn the complex on. While it certainly binds, we find no emission in β-CD even in the presence of cosolvents, which should help displace water from the cavity. Apparently, dppz is so sensitive to water that the range of applications where it will function as a dip stick is limited.

6.2. Polarity

A common problem is to assess the polarity of a solvent or of a binding environment. Pyrene has been the traditional probe for this. It has a sharp, highly structured emission, and the ratio of the different vibronic emission peaks is highly dependent on the local environment [76]. A number of other organic molecules with intramolecular charge transfer excited states have emission yields and spectra that are very sensitive to local polarity. These include organic molecules like Prodan and Patman, which can have twisted CT excited states.

Since the absorption and emission spectra of a number of transition metal complexes are highly dependent on solvent polarity, one might expect that they too would prove valuable probes. In practice, this has not yet been true, and the reasons for this failure are uncertain. For example, $RuL_2(CN)_2$ and $RuL(CN)_4^{2-}$ are extraordinarily sensitive to changes in bulk solvent. This is a result of the very asymmetric excited state, which has a large dipole moment change on going from the ground to the excited state. In spite of these huge binding shifts when varying the bulk solvent, binding of either complex to micelles where the local environment is radically different from bulk water yields no significant shifts in absorption or emission [77].

At this time, it is not clear that there are any suitable platinum metal diimine complexes for use as polarity probes in microheterogeneous systems. This may change as new complexes are discovered. An understanding of the precise nature of the nonlinear behavior of these metal complexes might prove useful in developing complexes that can overcome the current limitations. One molecule that might prove to be interesting in low temperature media is *trans*-$Pt(PEt_3)_2$(acetylide)$_2$. This complex exhibits an enormous variation in its site selectivity emission spectra and strong site selectivity [78].

6.3. Rigidity probes

An important area of interest is the rigidity of materials. This is of keen interest to those studying the curing of polymeric systems. Transition metal complexes have proved a powerful tool for studying, in real time, the curing of polymers. It had long been known that the sharpness and energy of many emission spectra are highly dependent on solvent rigidity. The most extreme examples of this are Shpol'skii spectroscopy where line-like emissions can be obtained from organic luminophores in a solvent where the solvent molecules and the luminophore have very similar sizes [79]. The basis of rigidity probes is as follows: if a molecule undergoes a large dipole moment change on excitation, the initially formed excited state finds itself in an environment where the solvent dipoles are oriented in an energetically unfavorable configuration. If the solvent relaxation times are shorter than the excited state lifetime, the environment and the excited state can relax before emission. This relaxation to the so-called thermally equilibrated excited state (*thexi*) can be at substantially lower energy than the initially excited molecule. When the relaxed species emits back to the ground state, the emission is to a

conformation of the molecule that has solvent dipoles that are in an orientation that is energetically most favorable for the excited state. This conformation is, of course, energetically unfavorable (i.e. at a higher energy) for the equilibrated ground state. Thus, the emission in a relaxed system will be at much lower energy than the 0–0 energy. However, if the molecule is in a rigid environment that cannot relax on a time scale of the excited state lifetime, the emission will be from the high energy, unequilibrated excited state to the initial conformation of the ground state. This emission will clearly be at higher energy than the emission in the low viscosity solvent.

Thus, for molecules having such large differences in energy between the initial and relaxed excited states, there will be large differences in emission spectra depending on the rigidity of the environment. Although such behavior was well known in many systems, the first use of the term *rigidochromic* was introduced for a series of Re(I) diimine complexes [19,20].

The rigidochromism of Re(I) complexes has been used to follow the changes in internal rigidity of polymers during the curing process [80]. This use of a molecular probe provides information about the internal dynamics that would be difficult or impossible to obtain by other techniques.

6.4. Water exposure

The degree of water exposure of a probe molecule is frequently a highly desirable quantity. This is true for binding sites in biopolymers, polymers, bilayers, and micelles. We have developed a very valuable method for directly measuring the degree of water exposure in binding of metal complexes to micelles, although the method is much more general and should be applicable to other systems. The method depends on the fact that OH vibrations of water are much more effective at quenching the metal complex excited states than are lower frequency OD vibrations of heavy water, D_2O. By comparing the lifetimes of the complex in H_2O and in D_2O in both the presence and absence of the binder, one can estimate the fraction of the surface of the sensor molecule exposed to the water solvent [81]. This approach was originally used for estimating coordination environment of rare earth ions in solution [82] and later in proteins [83].

The approach has limitations with $Ru^{II}L_3$ type complexes. It works best with electronically symmetrical excited states where the excitation can reside uniformly over all three ligands. If the excitation resides preferentially in one ligand, then the sampling of the environment is not uniform and the analysis can be weighted towards the environment around the preferentially excited ligand. Thus, all three ligands should be electronically the same or similar. Another place where the method can yield misleading results is if the local binding environment has exchangeable protons on OHs. The rate of energy transfer quenching can be different for these OHs than for water, and if the probes sample these OHs it can give misleading results. For example, in cyclodextrin binding studies, the hydroxyls on the open binding face of the CDs behave differently than water OHs. Our method can then miscount the water exposure. Nevertheless, the water exposure

method is a valuable tool for studying water environment around metal complex probes [84].

6.5. Dynamics

Determining the local viscosity and range of motions available to molecules bound to proteins, DNAs, other biopolymers, and vesicles and bilayers is an exceptionally important mechanistic and fundamental tool for the biochemist [34]. Dynamic polarization measurements provide a method. One excites the probe with polarized light and, in effect, monitors the time dependence of the polarized emission of a bound species. This can be done either by pulsed or by phase methods. Both provide similar information. The method hinges on the excited state lifetime being comparable to the rotational correlation times. If rotation is too slow, the emission will show no depolarization during the decay. If the rotation is too fast, the emission will be depolarized before the decay proceeds appreciably and no information is available. Thus, different lifetime probes effectively have different time scales that they can measure. Organic fluorophores typically have lifetimes in the 1–20 ns range, which make them useful for looking at motions of small biomolecules and localized motions in larger molecules. However, for really large molecules such as large proteins, viruses, and DNAs, the information is limited by lifetime. Luminescent TMC provides ideal dynamic polarization probes for these larger systems since their lifetimes are in the 0.1–100 μs range.

To date, studies in such large systems have been limited, but it is clear from the available data that this is a rich and productive field of study. For example, Ru(II) complexes have been used to study horse serum albumin proteins [58] and DNA [85].

7. Problem areas

7.1. General issues

There are several substantial problems currently associated with the use of luminescent TMCs in sensor and probe technology. These include photostability, ease of optical excitation, attachment chemistry, mixed sensor responses, understanding support–substrate interactions, and the exceptionally difficult problem of interpreting complex systems. We will give a brief overview of these difficulties.

7.2. Photostability

In addition to the problem of sensor stability with time and varying conditions, optical based sensors have the nagging problem of photostability or decomposition on extended exposure to light. This issue is exacerbated by the fact that the response depends on exciting the sample. As many of the sensors are designed for use in fiber optic systems, the sensor is small and relatively few molecules must

handle the high light exposures necessary for adequate signal-to-noise ratio. Thus, even what would be considered high photochemical stability can yield serious decomposition on extended use. Several strategies are used to minimize this problem. In general, the light source is on only during the measurement to minimize light exposure. Lifetime versus intensity measurements are significantly less prone to signal changes due to decomposition. For an intensity based measurement, a 20% decomposition would yield a 20% reduction in signal without any change in the analyte concentration. While in a lifetime measurement, the reduced intensity would give a somewhat lower S/N but would have no direct effect on the lifetime. Of course, some measurements have less demanding *stability* standards. A sensor on a patient in a critical care unit might only be used for a day or two and sensor replacement would be straightforward for a longer period; a sensor monitoring oxygen in a fermenter or a sewer plant might easily be expected to continue working for a year or more.

However, the best solution is to develop more stable sensors. Dürr [86] has claimed greater stability for pendant Ru(II) complexes with long polyethyleneoxide attachment, but no quantitative data are provided. It is possible that the long tails entangle the ligands and prevent rapid loss of ligand on photodissociation. A longer residence time would then permit self-healing by reattachment of the ligand. Os(II) sensor molecules promise higher photochemical stability than their Ru(II) analogues. Much of the Ru(II) photochemistry arises from ligand dissociation via the higher energy d–d state. Anything that raises the dissociative d–d relative to the MLCT emitting state will enhance photochemical stability. Osmium has a higher effective crystal field strength than Ru(II) and the emissive MLCT excited states are lower. Both of these factors increase the stability in solution. Whether this enhanced stability is carried over into polymer supported systems remains to be seen. This is not a foregone conclusion. For example, we have found that $ReL(CO)_3CN$ complexes are exceptionally robust in solution, and yet degrade photochemically very rapidly in the polymer supports that we have tested. Also, exceptionally high luminescence yields are not a guarantee of high stability. $ReL(CO)_3NCR^+$, which are some of the most highly emissive diimine complexes reported to date, appear to be much too unstable for practical sensors.

7.3. Excitability

A major shortcoming of Ru(II) and Re(I) sensors is that they generally must be excited in the blue and UV regions, respectively. These have traditionally been difficult regions for low-cost excitation sources, especially those that are employed in fiber optic probes where small source size and relative high intensity are important.

New high intensity blue LEDs are reducing the difficulty for blue excitation. Violet LEDs should be available shortly. Compact frequency tripled YAGs help in the UV, but the cost is still significant. Inexpensive frequency-doubled red and near IR laser diodes are promised in the near future. There is enormous commercial pressure for this last development. Current audio/video CD technology uses

670–800 nm diode lasers. Current information storage density is limited by the diffraction limit of the wavelength. Doubling this frequency gives half the wavelength, half the addressable size, and four times the information packing density. The fallout for the scientist will be great indeed.

The final approach is chemical. Find probes that absorb in the 635–780 nm region of very efficient, low cost, red, near-IR laser diodes. Osmium complexes analogous to the ruthenium sensors have been shown to be good prospects in this area [87,88]. The down sides are that they have shorter lifetimes and lower luminescence yields than analogous Ru(II) complexes. This is due to the smaller energy gap between the ground state and the emitting state for the Os(II) complexes, which increases the non-radiative quenching rate constant to the ground state. However, we have found one polymer–complex combination that has a 4.5-fold change in the emission intensity and lifetime on going from no oxygen to one atmosphere of pure oxygen. This is very functional for physiological measurements. New ligand systems will certainly prove valuable in enhancing performance of osmium complexes, either by just protecting the excited state from quenching or by better tuning the energy gap to the ground state while maintaining good excitability by red diode lasers.

Thus, it seems likely that the problems of excitability will steadily be overcome by a combination of better instrumentation at reduced cost and by enhanced photophysical properties. The current problems all seem like minor stumbling blocks on the way to highly successful utilization of a variety of different complexes.

7.4. Attachment

The problem of attachment to substrates is an issue of critical importance. One must design the necessary chemistry into the metal complex to allow attachment to the target. Since the ligands are generally organic, all of the tools currently used to attach organic probes should be equally applicable to metal complexes. Some of the reactive groups for attachment include isothiocyanates, acid anhydrides, sulfonyl chlorides, and acid chlorides. In addition, in polymeric systems, vinyl groups can also be added to provide a moiety for copolymerization with the polymer itself. Chemists are now beginning to apply the vast array of available synthetic tools for fabricating ligands that covalently attach to suitable targets.

In addition to covalent attachment, intercalation, ionic attraction, hydrophobic interactions, and guest–host interactions all provide means of attaching probes to suitable substrates. Because of the nature of the attachment, such techniques must necessarily be weaker than covalent systems. However, this does not preclude their very successful utilization. Indeed, many of the widely used organic probes use these binding modes. For example, a wide variety of intercalating dyes are used in DNA fingerprinting and sequencing down to, and including, the single molecule levels. Hydrophobic interactions are widely used for binding of membrane probes (e.g. 1,6-diphenyl-hexatriene). Again, these are just synthetic problems to create the suitably modified metal complex so that it binds tightly enough to the substrate by the appropriate mode.

Intercalating metal complexes have been very successfully used as described earlier. We have used hydrophobic/ionic interactions to tightly bind metal complexes to vesicle bilayers. So it seems likely that all of the strategies currently used with organic sensors and probes should be applicable.

7.5. Mixed responses

The very feature that makes the inorganic complexes so valuable is also their major weakness. The long excited state lifetimes make them susceptible to interferences by other species. A serious problem is that the complexes can show mixed responses to multiple components in the system. In particular, all of the long lived complexes show significant oxygen quenching. If one is analyzing anything but oxygen, this can be a major interferent. For example, a pH sensor in a biological system would be responding to both the pH changes and changes in local oxygen tension in the blood or tissue.

It is not obvious at this time how to circumvent this problem. Re(I) and Ir(II) complexes are substantially less sensitive to oxygen quenching than Ru(II) and Os(II) complexes of comparable lifetimes.

While not yet demonstrated, it may be possible to put an oxygen-impervious barrier around the non-sensing portion of the metal complex. The reduced oxygen quenching of metal complexes in some polymers may be a consequence of the complex being partially surrounded by an oxygen-impervious region of the polymer that does not allow oxygen close enough to the excited portion of the complex to quench it. Complexes with suitably engineered oxygen-impervious foliage on the ligands might achieve this shielding while leaving the sensing portion of the molecule (e.g. COOH on a bpy) exposed to the external environment where it can sense the analyte. Things that might help would be using asymmetric ligand combinations where the excitation resides in the shielded portion of the complex. This has been demonstrated with Re(I) complexes where, if the α-diimine portion of the complex is covered by the cyclodextrin, the oxygen shielding is very efficient; if the CD binds to an unexcited portion of the molecule, then quenching is only slightly reduced due to one side of the molecule being blocked from the approaching oxygen. Suitable shielding groups might be covalently bound CDs, alkanes, and polyethylene oxides.

7.6. Substrate–support interactions

One of the major difficulties of sensor design has been a clear understanding of the support–probe interactions. Especially in such areas as optical sensors, the interactions of the sensor molecule and the polymeric support play a critical role in performance. The support system can show complex variations in microstructure and the precise distribution of probe molecules within this microheterogeneous systems are quite complex. We have examined a variety of systematically varied polymer systems with different quenchometric oxygen sensors [89,90]. The behavior is quite complex, but several points were made. In many cases a domain structure

is a useful tool for predicting behavior of copolymers. Compatibility of the polymer with sensor molecules was critical, and mixed polymers could be used to create polar domains in otherwise non-polar polymers that would solubilize polar probes. Favorable mechanical characteristics and good oxygen quenching could be maintained by proper mixtures of copolymers. Some polymer systems were so delicately poised that as little as 0.5 wt% of a crosslinker additive could radically alter the behavior. We believe we can rationalize these results in that the two-site model for intensity quenching always seems to quantitatively fit the luminescence quenching behavior. However, our understanding is not to the point where we can reliably predict the properties of new sensor–polymer combinations.

We are currently developing fluorescence microscopy to better understand the interactions of the metal complexes with the polymer support. This is proving especially informative in studies of the heterogeneity of oxygen sensors [91].

Unfortunately, there are several areas where much more work is required. Support interactions of Re complexes, which should be good oxygen sensors, are largely unpredictable [92]. Partitioning behavior of the probe into different domains is complex and hard to predict. In many systems lifetime quenching data is complex and good models are difficult to develop.

In summary, it appears that the area of polymer–sensor design and modeling is very much in its infancy. Most of the work has focused on sensor support interactions for oxygen sensors and, to date, people have only looked at quenching based on external oxygen pressures. However, the more fundamental question of solubility and fundamental rate constants within the polymer still remain unanswered. How polymer structure affects diffusion within the polymer, a critical factor in response time, is still unknown. These issues, coupled with the necessary modeling and synthetic issues, are very exciting and one can look forward to enormous advances.

7.7. The uniqueness problem

As has long been recognized it is extremely difficult to accurately fit experimental decay curves to sums of exponentials, especially for relatively close lifetimes (< factor of 2) [93,94]. However, the point is so important that it justifies repeating. We present an even more extreme case [95]. To help appreciate the difficulty, we consider five functions. The first is given by a Gaussian distribution of lifetimes with a center lifetime of 15 and a standard deviation on the width of 3.75. The scaling factor was adjusted to give a decay curve with a peak of 10^4. This is an extremely wide distribution; any wider distribution would have a substantial intensity at $\tau < 0$, which seems chemically unreasonable. We define this function as $D_G(t)$. The remaining four functions are

$$D_1(t) = 4582.5 \exp(-t/11.092) + 5395.3 \exp(-t/18.379) \quad (6a)$$

$$D_2(t) = 2005.7 \exp(-t/7.6144) + 8022.8 \exp(-t/16.774) \quad (6b)$$

$$D_3(t) = 7910.7 \exp(-t/13.434) + 1977.9 \exp(-t/21.179) \quad (6c)$$

$$D_4(t) = 702.2\exp(-t/6.977) + 5892\exp(-t/13.223) + 3406\exp(-t/19.72) \quad (6d)$$

Initially, it is hard to imagine such dissimilar functions. While D_1, D_2, and D_3 are all double exponential decays, their pre-exponential factors deviate radically and the lifetimes differ noticeably. The ratio of pre-exponentials for the fast and slow components vary by a factor of 16! D_1 has comparable amplitudes, while D_2 has a ratio of short to long of 4, and D_3 has a ratio of long to short of 4. D_4 is a sum of three exponentials. All five functions vary from a peak of about 10^4 to 25, and all four functions, if overlaid, are virtually indistinguishable. To amplify these differences, we assume that the Gaussian distribution, D_G, is the correct decay function and examine the deviations of the other functions from D_G. In all cases the double exponential D_1 fits the distribution decay essentially perfectly. Even D_2 and D_3 were very credible fits. D_4 matches D_G so well that the differences are invisible on the same scale as the others.

To better appreciate the indistinguishability of these functions, we compared the differences between D_G and these functions with the error bounds of $\pm\sigma$ assuming that the data came from a single photon counting (SPC) lifetime instrument (Poisson statistics). In all cases the instrument's Poisson noise greatly exceeded the differences. Thus, for 10^4 peak counts in SPC data, differentiation between any of these functions is virtually experimentally impossible. Experimental noise hides the differences. Obviously, there is a continuum of possible lifetimes and preexponential factors that would be similarly indistinguishable.

We have also shown several other places where the ambiguity problem can make a unique interpretation impossible; this includes the case of a double Gaussian distribution of lifetimes. The reader is referred to the original papers [96].

Another somewhat different example of the dangers of drawing mechanistic conclusions from uncritical modeling is shown by the two common models used for fitting intensity quenching data in polymers. In one model, the sensor is treated as existing in two discrete sites each with a different Stern–Volmer quenching constant. In the second, each molecule is assumed to be equivalent, but the solubility of oxygen in the polymer is assumed to be nonlinear and to obey the common nonlinear solubility equation for gases in glassy polymers.

For a two-site model, the simplest form that gives a nonlinear Stern–Volmer equation, we have [97],

$$\left(\frac{I_o}{I}\right) = \frac{1}{\dfrac{f_{01}}{1+K^p_{SV1}p_{O_2}} + \dfrac{f_{02}}{1+K^p_{SV2}p_{O_2}}} = \frac{1}{\dfrac{f_{01}}{1+K^p_{SV1}p_{O_2}} + \dfrac{1-f_{01}}{1+K^p_{SV2}p_{O_2}}} \quad (7)$$

where I is the normal Stern–Volmer intensities, f is the fractional contributions to the unquenched emissions, K is the different Stern–Volmer quenching constants expressed in pressure units, and p is the oxygen pressure. A two-component system is a three-parameter model since $f_1 + f_2 = 1$.

For the three parameter nonlinear gas solubility model, we have

$$\left(\frac{I_o}{I}\right) = 1 + Ap_{O_2} + \frac{Bp_{O_2}}{1 + bp_{O_2}} \quad (8)$$

where A and B are composite parameters including gas solubility parameters and rate constants, and b is the parameter in the nonlinear gas solubility equation [98].

In spite of the fact that these two equations are completely different and have radically different physical interpretations, it turns out that they are mathematically absolutely equivalent [97]. That is, fitted nonlinear Stern–Volmer plots will be fit exactly as well by each equation! While we believe there are good reasons (based on other evidence) to favor the two site approximation over the nonlinear gas solubility model in elastomer supports, there is no way to distinguish between the models just on the intensity quenching data.

In summary, the uniqueness problem is so severe in luminescence decay measurements in microheterogeneous systems that frequently one cannot reliably discern the difference between a simple distribution of lifetimes or a sum of two or three exponentials under many experimentally realizable conditions. Further, even assuming that the decay is a known double exponential, one can be hard pressed to determine the major component without recourse to more exotic instrumentation than is readily available.

While irritating from a fundamental point, this difficulty or inability to critically determine mechanistic details is not crippling for practical devices. Indeed, for real sensors one would like to reduce the complexities to a single unique number, which is monotonically dependent on the analyte concentration. The rapid lifetime determination method [99] and the phase shift methods are quite good at hiding this complexity [34]. However, even for mechanistic studies such tools as global fitting of multiple parameter sets can be extremely useful at tying down a complex scheme or at least minimizing the number of viable models.

Acknowledgements

The authors wish to thank the National Science Foundation (CHE-94-19074 and CHE 97-26999) and Ford Motor Company for their support.

References

[1] K. Kalyanasundaram, Coord. Chem. Rev. 46 (1982) 159.
[2] K. Yamashita, S. Yamazaki-Nishida, Y. Harima, A. Segawa, Anal. Chem. 63 (1991) 872.
[3] N.E. Tokel-Takvoryan, R.E. Hemingway, A.J. Bard, J. Am. Chem. Soc. 95 (1973) 6582.
[4] T.D. Tullius (Ed.), Metal–DNA Chemistry, ACS Symposium Series 401, American Chemical Society, Washington, DC, 1989.
[5] E. Tsuchida (Ed.), Macromolecular Complexes Dynamic Interactions and Electronic Processes, VCH, New York, 1991.
[6] A. Sobczynski, A.J. Bard, A. Campion, M.A. Fox, T. Mallouk, S.E. Webber, J.M. White, J. Phys. Chem. 91 (1987) 3316.

[7] K. Kalyanasundaram, Photochemistry in Microheterogeneous Systems, Academic Press, New York, 1987.
[8] J. Chem. Educ. 74 (1997) Entire issue.
[9] R.J. Watts, J. Chem. Educ. 60 (1983) 834, and references therein.
[10] J.N. Demas, B.A. DeGraff, P.B. Coleman, Anal. Chem. 71 (1999) 793A.
[11] P.C. Ford, Rev. Chem. Intermed. 2 (1979) 267.
[12] C. Creutz, M. Chou, T.L. Netzel, M. Okimura, N.J. Sutin, J. Am. Chem. Soc. 102 (1980) 1309.
[13] G.A. Reitz, J.N. Demas, E. Stephens, B.A. DeGraff, J. Am. Chem. Soc. 110 (1988) 5051.
[14] L. Sacksteder, J.N. Demas, B.A. DeGraff, Inorg. Chem. 28 (1989) 1787.
[15] E.M. Kober, J.L. Marshall, W.J. Dressick, B.P. Sullivan, J.V. Caspar, T.J. Meyer, Inorg. Chem. 24 (1985) 2755.
[16] R.J. Watts, B.G. Griffith, J.S. Harrington, J. Am. Chem. Soc. 98 (1976) 674.
[17] A.J. Lees, Chem. Rev. 87 (1987) 711.
[18] J.V. Caspar, B.P. Sullivan, T.J. Meyer, Inorg. Chem. 23 (1984) 2104.
[19] M.S. Wrighton, D.L. Morse, J. Am. Chem. Soc. 96 (1974) 998.
[20] P.J. Giordano, M.S. Wrighton, J. Am. Chem. Soc. 100 (1979) 2888.
[21] J.N. Demas, B.A. DeGraff, Anal. Chem. 63 (1991) 829A.
[22] L. Sacksteder, M.M. Lee, J.N. Demas, B.A. DeGraff, J. Am. Chem. Soc. 115 (1993) 8230.
[23] F.A. Cotton, G. Wilkinson, Advanced Inorganic Chemistry, Wiley, New York, 1980 (Chapter 20).
[24] J.N. Demas, G.A. Crosby, J. Am. Chem. 93 (1971) 2841.
[25] H.J. Hough, J.N. Demas, T.O. Williams, H.N.G. Wadley, Acta Metal. Mater. 43 (1995) 821.
[26] D.R. McMillan, K.M. McNett, Chem. Rev. 98 (1998) 1201.
[27] S.D. Cummings, R. Eisenberg, Inorg. Chem. 34 (1995) 3396.
[28] S.D. Cummings, R. Eisenberg, Inorg. Chem. 34 (1995) 2007.
[29] K. Mandel, T.D.L. Pearson, J.N. Demas, J. Chem. Phys. 73 (1980) 2507.
[30] J.V. Caspar, E.M. Kober, B.P. Sullivan, T.J. Meyer, J. Am. Chem. Soc. 104 (1982) 630.
[31] J.V. Caspar, T.J.J. Meyer, Phys. Chem. 87 (1983) 952.
[32] L. Sacksteder, A.P. Zipp, E. Brown, J. Streich, J.N. Demas, B.A. DeGraff, Inorg. Chem. 29 (1990) 4335.
[33] R. Grigg, J.M. Holmes, S.K. Jones, W.D.J.A. Norbert, J. Chem. Soc. Chem. Commun. (1994) 185.
[34] J.R. Lakowicz, Principles of Fluorescence Spectroscopy, Plenum, New York, 1983.
[35] O.S. Wolfbeis, in: O.S. Wolfbeis (Ed.), Fiber Optic Chemical Sensors and Biosensors, vol. 2, CRC Press, Boca Raton, FL, 1991, pp. 19–53 (Chapter 10).
[36] J.R. Bacon, J.N. Demas, Anal. Chem. 59 (1987) 2780.
[37] E.R. Carraway, J.N. Demas, B.A. DeGraff, J.R. Bacon, Anal. Chem. 63 (1991) 337.
[38] K.A. Kneas, W. Xu, J.N. Demas, B.A. DeGraff, J. Chem. Educ. 74 (1997) 696.
[39] S.H. Peterson, J.N. Demas, J. Am. Chem. Soc. 98 (1976) 7880.
[40] P.J. Giordano, C.R. Bock, M.S. Wrighton, J. Am. Chem. Soc. 100 (1978) 6960.
[41] R. Grigg, W.D.J.A. Norbert, J. Chem. Soc. Chem. Commun. (1992) 1300.
[42] W. Xu, J. Mehlmann, J. Rice, J.E. Collins, C. Fraser, J.N. Demas, B.A. DeGraff, M. Bassetti, SPIE Conf. Environ. Monit. Remediat. Technol. 3534 (1998) 456.
[43] J.N. Demas, Excited State Lifetime Measurements, Academic Press, New York, 1983.
[44] U. Kosch, I. Klimant, T. Werner, O.S. Wolfbeis, Anal. Chem. 70 (1998) 3892.
[45] C. Huber, T. Werner, C. Krause, I. Klimant, O.S. Wolfbeis, Anal. Chim. Acta 364 (1998) 143.
[46] O.S. Wolfbeis, in: S.G. Schulman (Ed.), Molecular Luminescence Spectroscopy Methods and Applications: Part 2, Wiley, New York, 1988, p. 283.
[47] A. Mills, Q. Ching, N. McMurray, Anal. Chem. 64 (1992) 1383.
[48] A. Mills, L. Wild, Q. Chang, Mikrochim. Acta 121 (1995) 225.
[49] N.P. Ayala, J.N. Demas, B.A. DeGraff, J. Am. Chem. Soc. 110 (1988) 1523.
[50] M.G. Kinnaird, D.G. Whitten, Chem. Phys. Lett. 88 (1982) 275.
[51] J.N. Demas, J.W. Addington, S.H. Peterson, E.W. Harris, J. Phys. Chem. 81 (1977) 1039.
[52] Y. Shen, B.P. Sullivan, J. Chem. Educ. 74 (1997) 685.
[53] C.S. Rawles, P. Moore, N.W. Alcock, J. Chem. Soc. Commun. (1992) 684.

[54] R.W. Harrigan, G.D. Hager, G.A. Crosby, Chem. Phys. Lett. 21 (1973) 487.
[55] J.N. Demas, B.A. DeGraff, SPIE 1796 (1992) 71.
[56] L.B. McGown, F.V. Bright, Crit. Rev. Anal. Chem. 18 (1987) 245.
[57] E. Terpetschnig, H. Szmacinski, J.R. Lakowicz, Anal. Biochem. 227 (1995) 140.
[58] H.J. Youn, E. Terpetschnig, H. Szmacinski, J.R. Lakowicz, Anal. Biochem. 232 (1995) 24.
[59] X.-Q. Guo, G.N. Catellano, L. Li, J.R. Lakowicz, Anal. Chem. 70 (1998) 632.
[60] J.M. Kelly, A.B. Tossi, D.J. McConnell, C. OhUigin, Nucl. Acids Res. 13 (1985) 6017.
[61] P.B. Dervan, Science 232 (1986) 464.
[62] W.A. Remers, Antineoplastic Agents, Wiley, New York, 1984.
[63] W.D. Wilson, R.L. Jones, in: M.S. Whittingham, A.J. Jacobson (Eds.), Intercalation Chemistry, Academic Press, New York, 1982, p. 445.
[64] H.W. Zimmermann, Angew. Chem. 98 (1986) 5.
[65] J.K. Barton, L.A. Basile, A. Danishefsky, A. Alexandrescu, Proc. Natl. Acad. Sci. USA 81 (1984) 1961.
[66] J.K. Barton, Science 233 (1986) 727.
[67] A.M. Pyle, J.P. Rehmann, R. Meshoyrer, C.V. Kumar, N.J. Turro, J.K.J. Barton, J. Am. Chem. Soc. 111 (1989) 3051.
[68] M.B. Fleisher, H.-Y. Mei, J.K. Barton, in: F. Eckstein, D.M.J. Lilley (Eds.), Nucleic Acids and Molecular Biology, vol. 2, Springer, Berlin, 1988, p. 65.
[69] S. Satyanarayana, J.C. Dabrowiak, J.B. Chaires, Biochemistry 31 (1992) 9319.
[70] J.E. Coury, J.R. Anderson, L. McFail-Isom, L.D. Williams, L.A. Bottomley, J. Am. Chem. Soc. 119 (1997) 3792.
[71] A.B. Tossi, J.M. Kelly, Photochem. Photobiol. 49 (1989) 545.
[72] H.-Y. Mei, J.K. Barton, J. Am. Chem. Soc. 108 (1986) 7414.
[73] J. Gorner, A.B. Tossi, C. Stradowski, D. Shulte-Frohlinde, Photochem. Photobiol. 2 (1988) 67.
[74] J. Fees, W. Kaim, M. Moscherosch, W. Matheis, J. Klima, M. Krejcik, S. Zalis, Inorg. Chem. 32 (1993) 166.
[75] R.E. Holmlin, E.D.A. Stemp, J.K. Barton, Inorg. Chem. 37 (1998) 29.
[76] K. Kalyanasundaram, J.K. Thomas, J. Am. Chem. Soc. 99 (1977) 2039.
[77] S.W. Snyder, S.L. Buell, J.N. Demas, B.A. DeGraff, J. Phys. Chem. 89 (1989) 5265.
[78] L. Sacksteder, E. Baralt, B.A. DeGraff, C.M. Lukehart, J.N. Demas, Inorg. Chem. 30 (1991) 2468.
[79] J.W. Hofstraat, C. Gooijer, N.H. Velhorst, in: S. Schulman (Ed.), Molecular Luminescence Spectroscopy — Methods and Applications: Part 2, Wiley-Interscience, New York, 1988, p. 283 (Chapter 4).
[80] T.G. Kotch, A.J. Lees, S.J. Fuerniss, K.I. Papathomas, R.W. Snyder, Inorg. Chem. 32 (1993) 2570.
[81] B.L. Hauenstein, Jr., W.J. Dressick, S.L. Buell, J.N. Demas, B.A. DeGraff, J. Am. Chem. Soc. 105 (1983) 4251.
[82] J.R. Kropp, M.W. Windsor, J. Phys. Chem. 71 (1967) 477.
[83] D.DeW. Horrocks, Jr., D.R. Sudnick, Acc. Chem. Res. 14 (1981) 384.
[84] J.I. Cline, III, W.J. Dressick, J.N. Demas, B.A. DeGraff, J. Phys. Chem. 84 (1985) 94.
[85] J.R. Lakowicz, H. Malak, I. Gryczynski, F.N. Castellano, G.J. Meyer, Biospectroscopy 1 (1995) 163.
[86] M. Seiler, H. Dürr, E. Joselevich, A. Doron, J.F. Stoddard, J. Am. Chem. Soc. 116 (1994) 3399.
[87] S.B. Bambot, G. Rao, M. Romauld, G.M. Carter, J. Sipior, E. Terpetchnig, J.R. Lakowicz, Biosens. Bioelectron. 10 (1995) 643.
[88] W. Xu, K.A. Kneas, J.N. Demas, B.A. Degraff, Anal. Chem. 68 (1996) 2605.
[89] J.N. Demas, B.A. Degraff, W. Xu, Anal. Chem. 67 (1995) 1377.
[90] K.A. Kneas, W. Xu, J.N. Demas, B.A. Degraff, Appl. Spec. 51 (1997) 1346.
[91] K.A. Kneas, J.N. Demas, A.H. Periasamy, B.A. DeGraff, submitted.
[92] K.A. Kneas, W. Xu, J.N. Demas, B.A. DeGraff, A.P. Zipp, J. Fluoresc. 8 (1998) 295.
[93] D.R. James, Y.-S. Liu, P. DeMayo, W.R. Ware, Chem. Phys. Lett. 120 (1985) 460.

[94] A. Seimiarczuk, W.R. Ware, J. Phys. Chem. 93 (1989) 7609.
[95] J.N. Demas, B.A. Degraff, Sensors Actuators B 11 (1993) 35.
[96] J.N. Demas, B.A. DeGraff, SPIE Opt. Based Methods Process Anal. 1681 (1992) 2.
[97] J.N. Demas, B.A. Degraff, W. Xu, Anal. Chem. 67 (1995) 1377.
[98] X.-M. Li, K.-Y. Wong, Anal. Chim. Acta 262 (1992) 27.
[99] K.K. Sharman, A.H. Periasamy, H. Ashworth, J.N. Demas, N.H. Snow, Anal. Chem. 71 (1999) 947.